Analysis of Base Heating Environment during Ground Testing of a Lunar Lander Demonstrator

Ten-See Wang, Francisco Canabal, Kyle Knox, and Robert Hawkins

NASA Marshall Space Flight Center, Huntsville, Alabama

and

Matt Bergman

Masten Space Systems, Mojave, California

66th JANNAF Propulsion Meeting (Unclassified)

June 3, 2019

Dayton Convention Center, Dayton, Ohio

Objective

- The objective of this study is to provide a four-engine clustered nozzle plume induced base heating environment for a lunar lander demonstrator, using a computational fluid dynamics and heat transfer methodology. Two cases were investigated.
  - Lunar lander demonstrator sitting on pad for the worst case.
  - Lunar lander demonstrator hovering at a distance above ground.

Introduction

- This lunar lander demonstrator, known as XL-1T (terrestrial), is a collaborative effort between Masten Space Systems and NASA, under NASA's Lunar CATALYST (also known as Lunar Cargo Transportation and Landing by Soft Touchdown) initiative.
- The lunar lander is a reusable terrestrial test bed for Masten's powered decent landing system, and will be controlled by four throttleable main engines utilizing green hypergolic propellants.
- One of the concerns for a four-engine vehicle like this demonstrator, is the potential for a severe base-heating environment, caused by the formation of a "fountain jet" during testing. Fountain jet is an unique base flow physics which was discovered during the development of the DC-X vehicle.

Previous studies – DC-X on-ground effect (1998)

- Gridgen was used to generate all hexahedral-cell grids (320,787 to 408,288 nodes). O-grid was used as surface grid for the nozzle exit plane which was extended all the way to the ground.
- O-grid cells are symmetric to the center of the nozzle. The entire hexahedral cells are symmetric to the centerline.
- FDNS structured-grid CFD code was used to compute the convective and radiative base heat fluxes.
- DC-X components were covered by an aeroshell which eliminated situation of flow over components, hence reduced flow instability from vortex shedding.

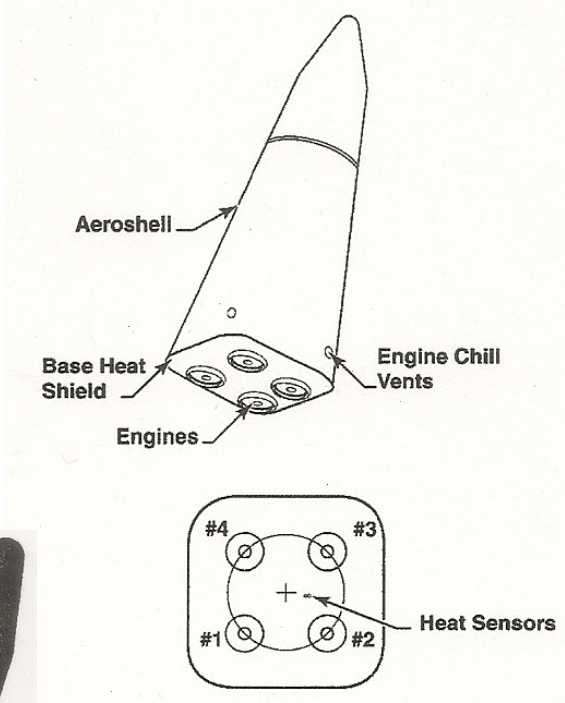

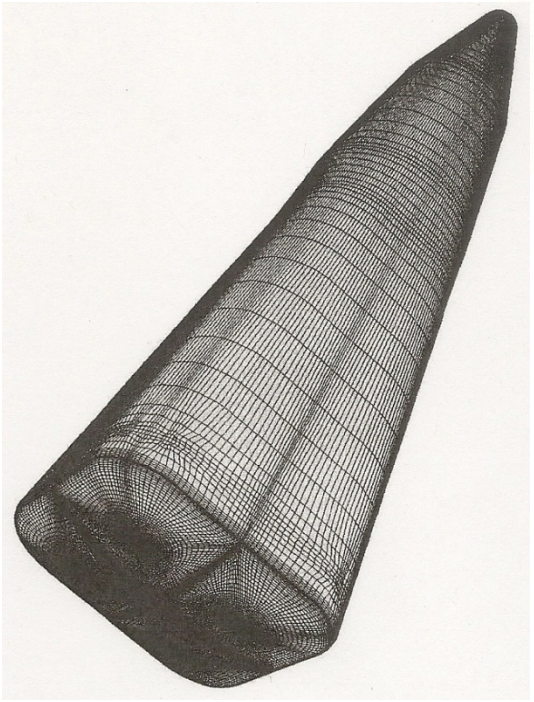

Previous studies – DC-X on-ground effect (1998)

- DC-X on-ground base flow physics captured:
  - Nozzle plume jets which impinges on the ground to form a ground jet.
  - The inward-going ground jet converges to form a fountain jet, which impinges on the base to form a base wall jet.
  - Air entrainment and plume afterburning
- Near convergence solutions show a symmetric flowfield and a stable fountain jet.
- Plume afterburning is one important physics for base heating prediction

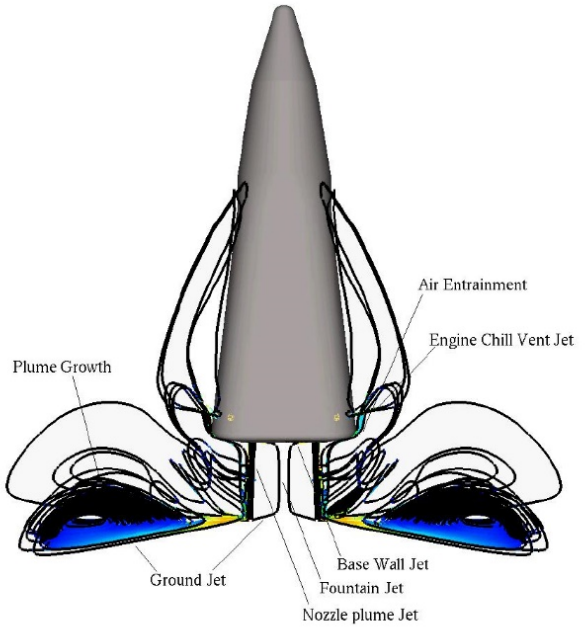

Qc/Qo

Coanda Effect

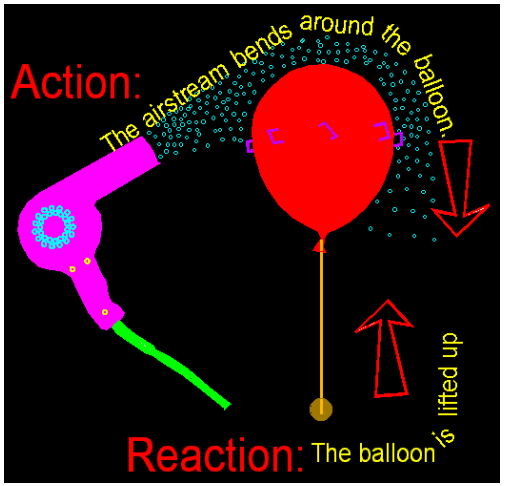

Coanda Effect in a Transient Nozzle

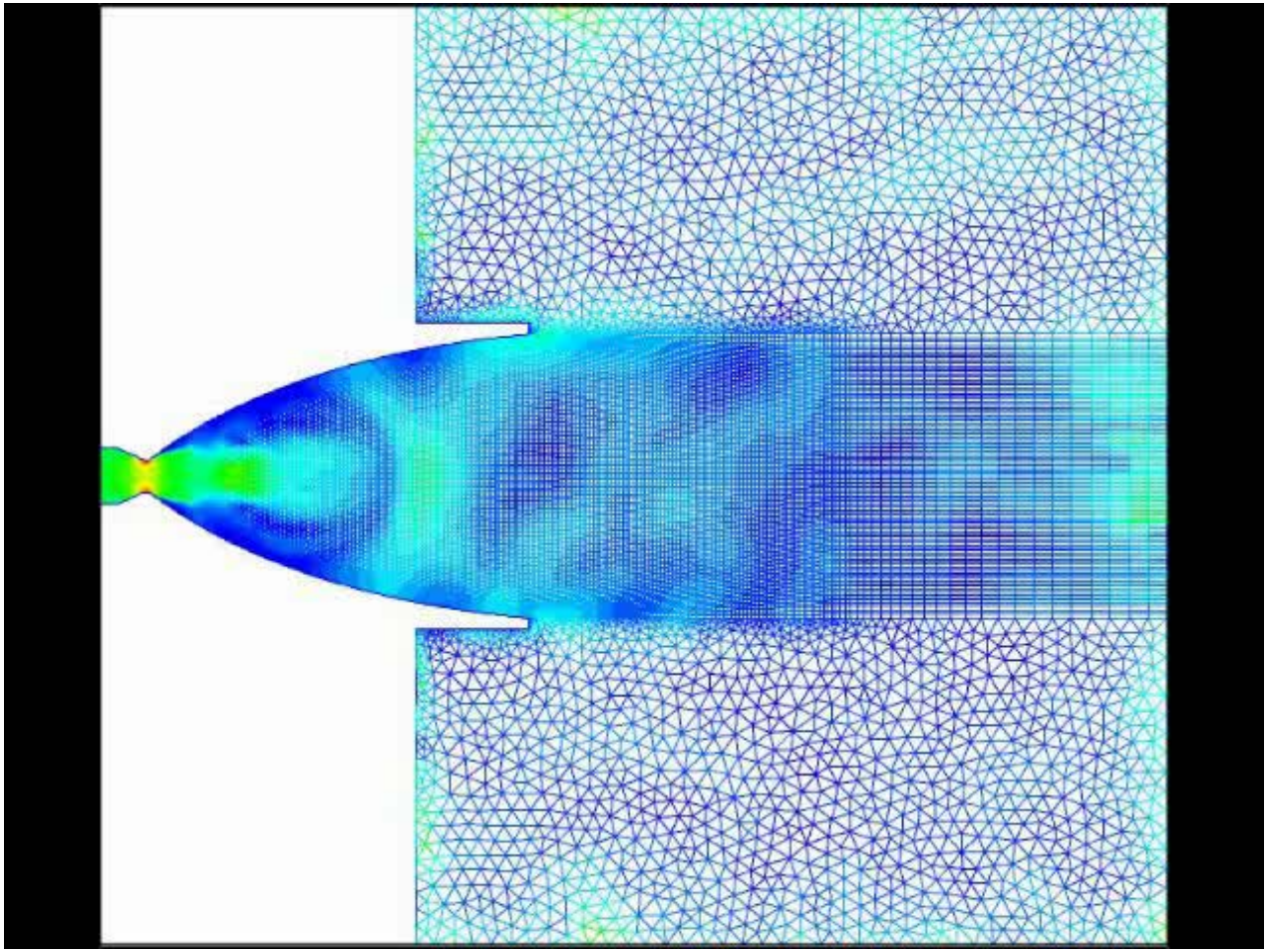

Flowfield and Radiation Codes

- UNIC CFD code
  - UNIC is a pressure-based, unstructured-grid, three-dimensional, turbulent and reacting, computational fluid dynamics and heat transfer code, capable of performing coupled radiation (Radiative Transport Equation) and conjugate heat transfer computations (FDNS CFD code is a structured-grid version of UNIC CFD code).
  - Weighted-sum-of-gray-gas model (WSGG) and spectral-line-based WSGG are available for radiation property calculations. WSGG model was used in this study.
- GASRAD radiation heat transfer code
  - GASRAD uses line-of-sight method integrated over a hemisphere to calculate radiative heat flux on vehicle body points receiving radiation from exhaust plumes (typically calculated from a separate flow model such as SPF-III). It uses a narrow-band model for radiation properties.
  - The SPF-III flowfield does not take into account plume/plume or plume/surface interactions. The complicated base flow physics such as fountain jet/base or plume-ground impingement cannot be easily modeled using such engineering methods. In order to account for those physics, two axisymmetric slices were extracted from the CFD solution: one for the fountain jet, another for the plume/ground interaction. These slices are then rotated and added into the nozzle plumes for the radiation calculation.

GASRAD thermo-flowfield arrangement

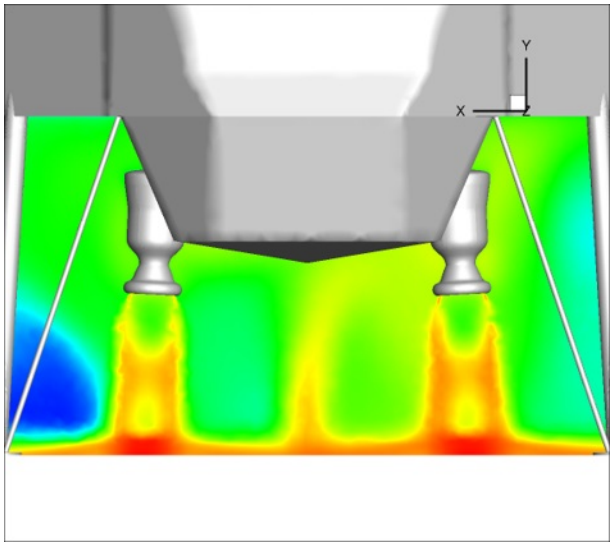

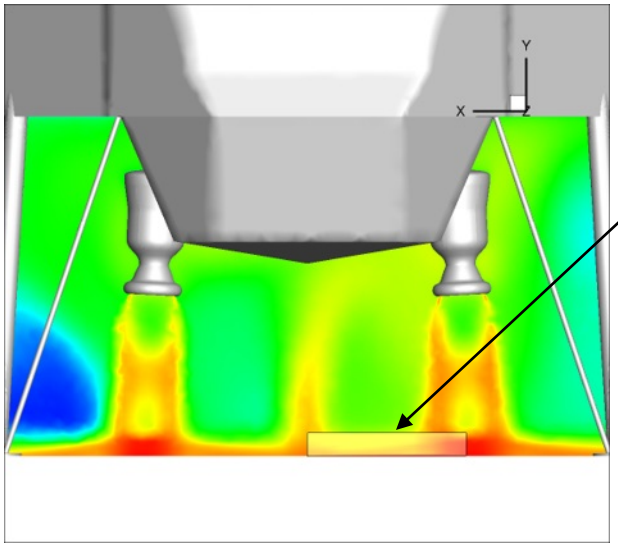

This section was Used to model stagnation regions.

GASRAD Stagnation Region at Nozzle Centerline

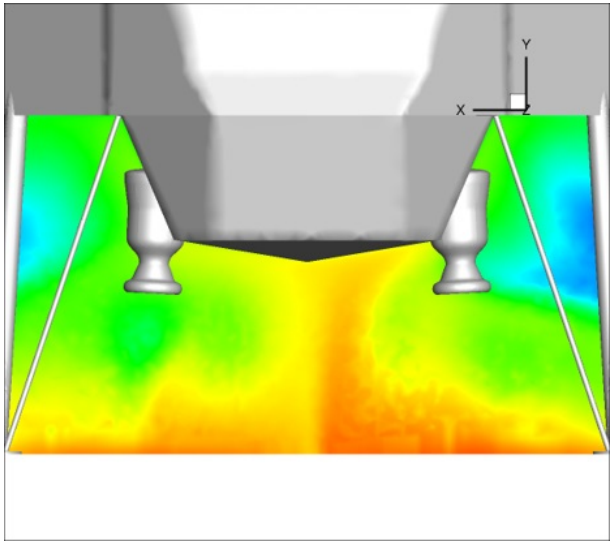

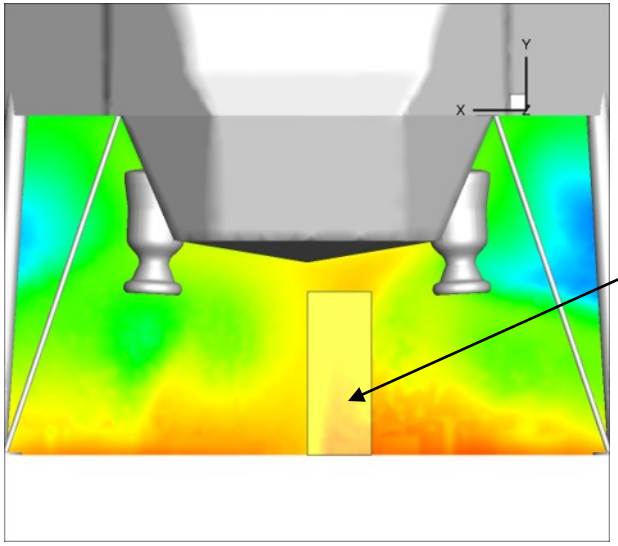

Hotter part of fountain jet was used to model the "high" heat flux modeling. "Low" heat flux was calculated using both the hotter and colder sections of the fountain jet.

GASRAD Fountain Jet Region at Base Center

Computational grid generation for the lunar lander demonstrator

- Started from a STEP CAD file
- ANSA was used to simplify and stitch in order to form a water-tight domain comprised of multiple faces
- ANSA was then used to generate surface mesh on the faces
- AFLR3 was used to generate volume mesh for CFD computations

Computational grid – Face meshes

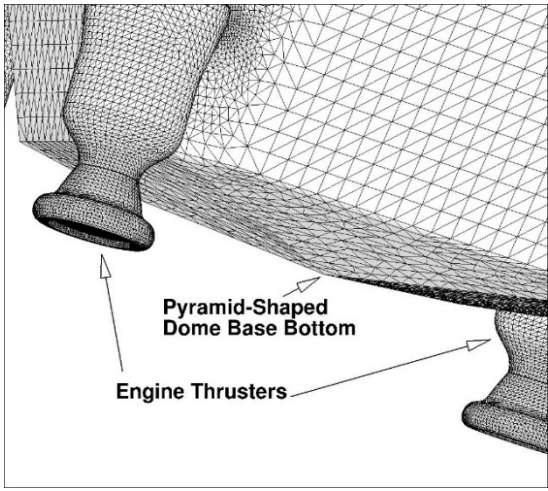

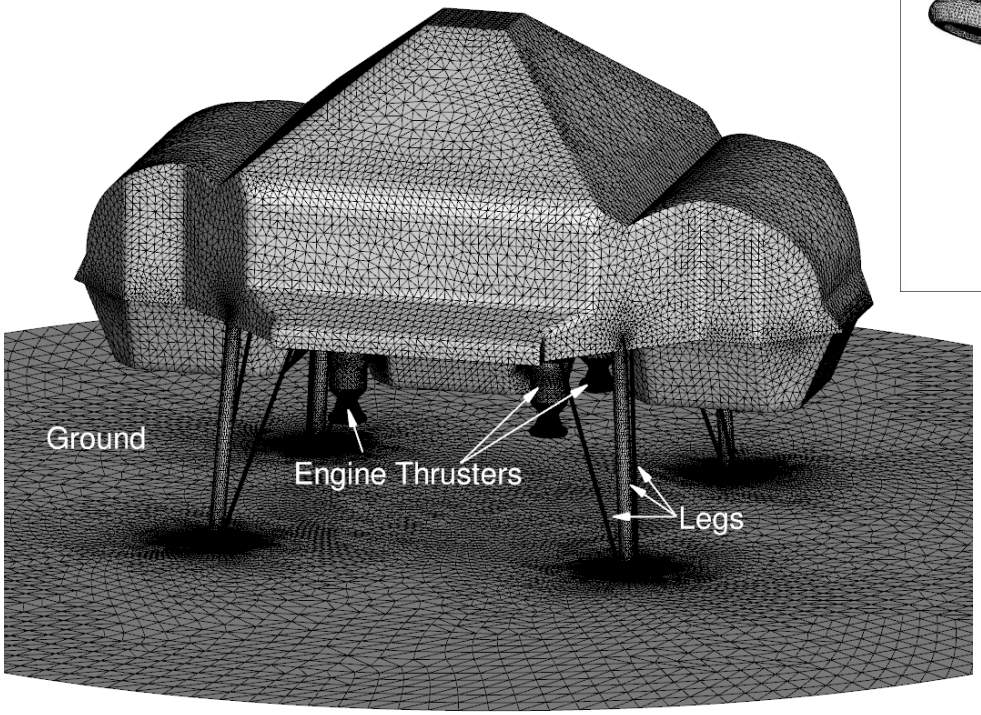

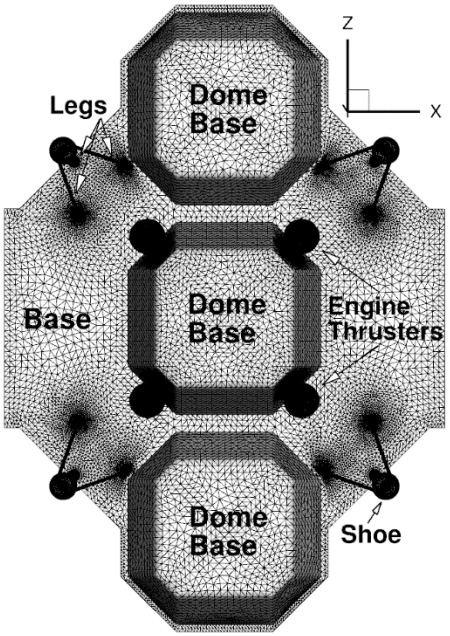

Grid 1: 12,979,470 cells

Computational grid – Initial face meshes improved by adding source cylinders in ANSA

- AFLR (Advancing Front Locally Reconnect) creates volume cells that are inherently asymmetric. Source cylinder allows local cell refinement inside itself, providing better resolution for important flow regions such as fountain jet and nozzle jets.

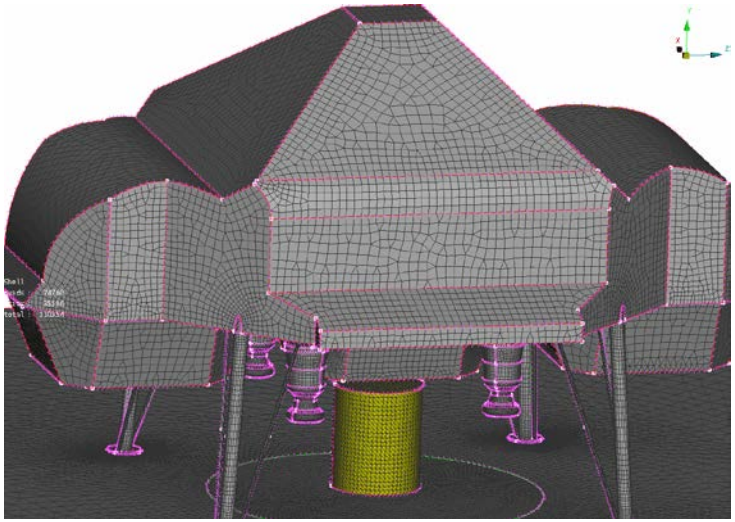

Grid 2: 15,926,621 cells

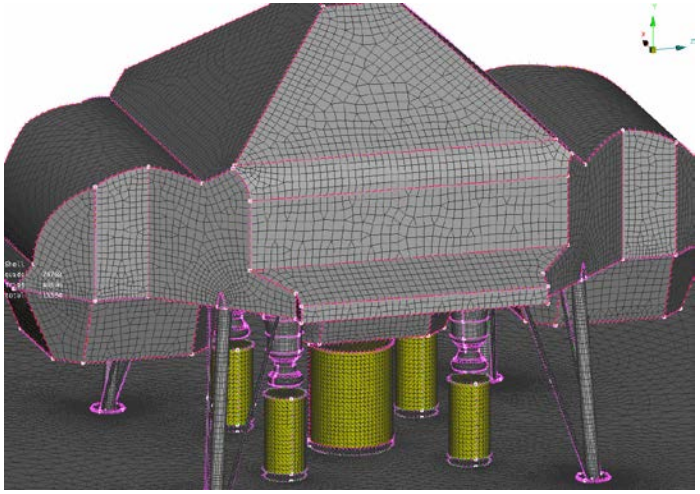

Grid 3: 13,843,266 cells

Engine plume inlet conditions

- Fuel: sodium and boron containing green propellants
  Oxidizer: hydrogen peroxide
- CEA was used to compute combustor flow properties. CEA calculation resulted in 17 species. By eliminating 3 trace species, 14 species are considered for CFD computations: H_2O, O_2, H_2, O, H, OH, CO, CO_2, HBO_2, $NaBO_2$, Na, NaOH, BO_2, N_2.

UNIC heat flux calculations

- Extended k-ε turbulence model was used with wall function. Equilibrium chemistry was used for plume afterburning.
- Convective and radiative heat fluxes were calculated with separate computations.
- Convective heat fluxes were calculated based on a wall temperature of 300 deg. K
- Radiative heat fluxes were calculated based on an adiabatic wall for conservative purpose. Adiabatic wall temperatures can be backed out readily if needed.
  - Two major radiators, H_2O and CO_2, were considered.
  - Emissivity of 0.85 (weathered steel) was assumed for the metal surface, while emissivity of 0.91 (clay) was assumed for the ground. This means radiation from both hot gas and surface are computed.

Results

Base heating environment for lunar lander sitting on pad

Pressure Contours

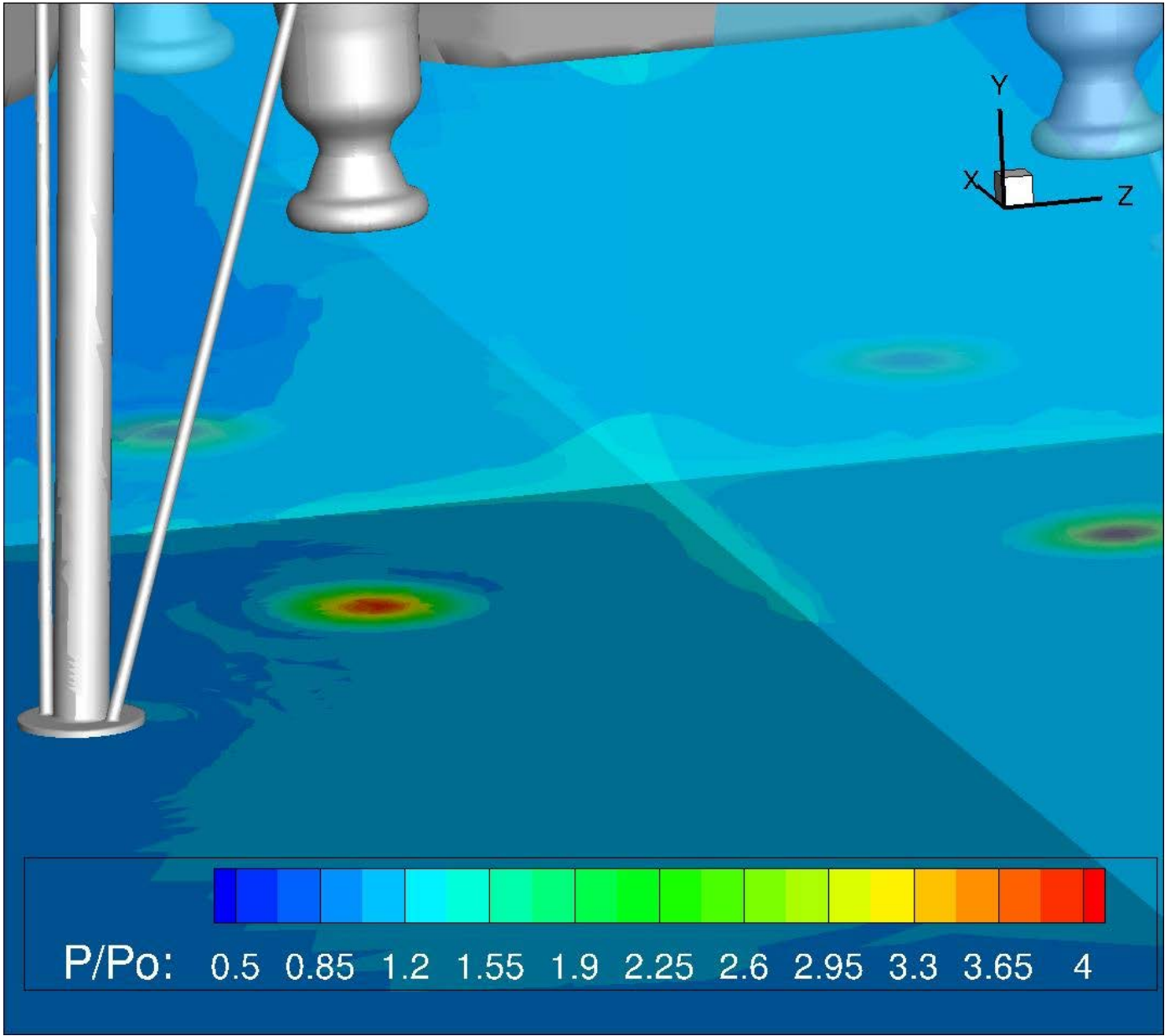

Temperature Contours

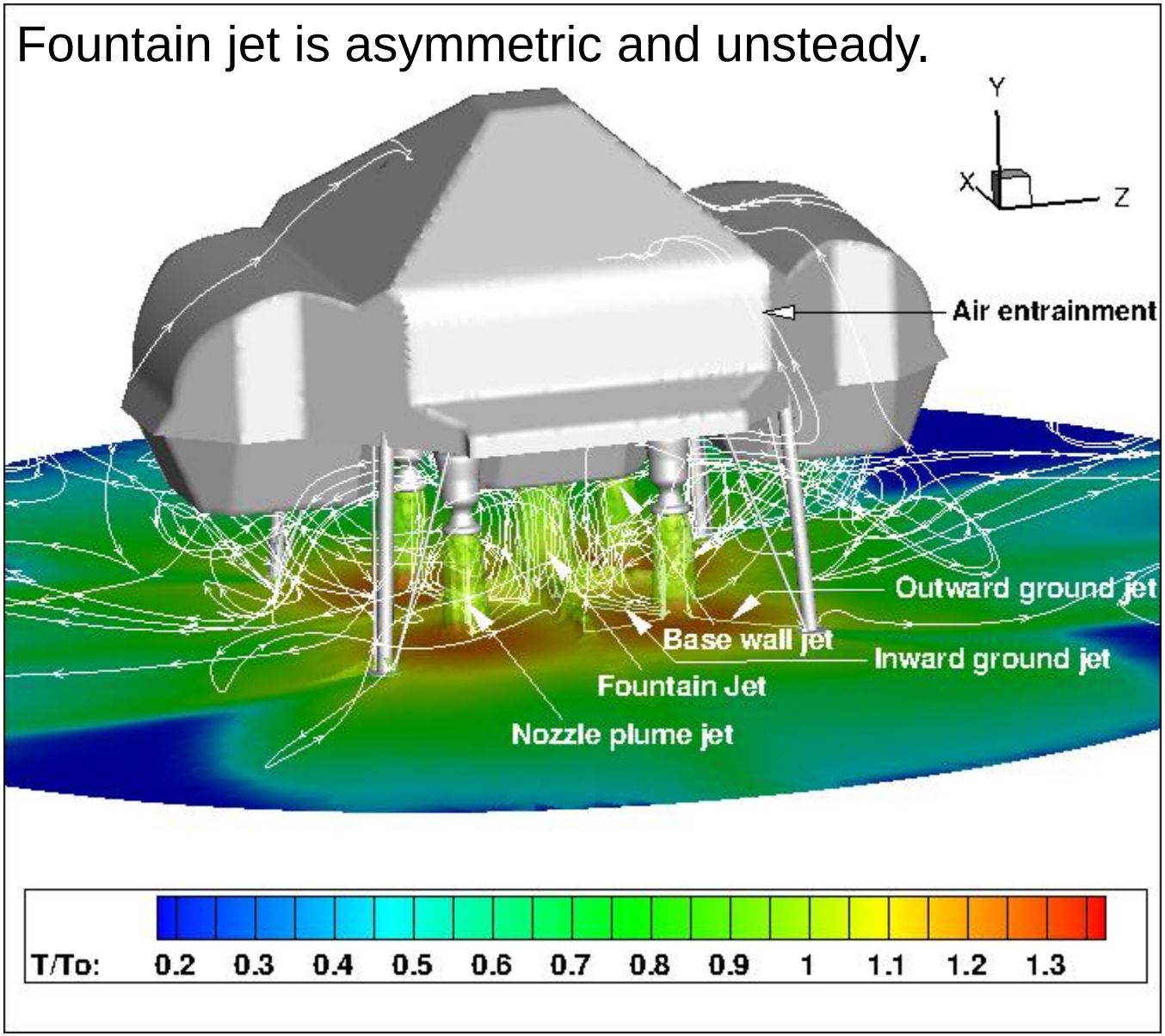

Base Convective Heat Flux Contours

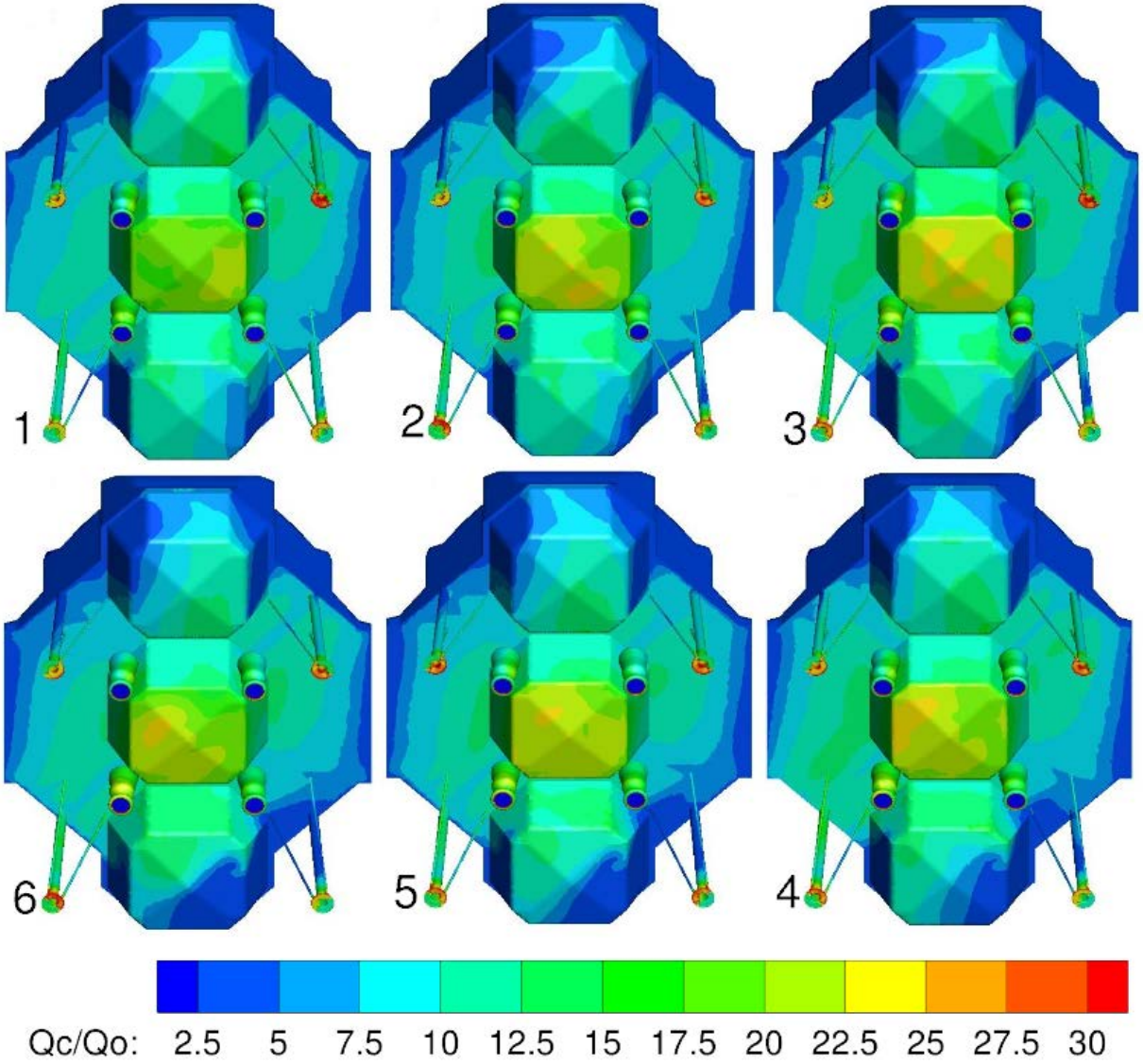

Contours show base convective heat flux variation over elapsed time.

Base Temperature Contours

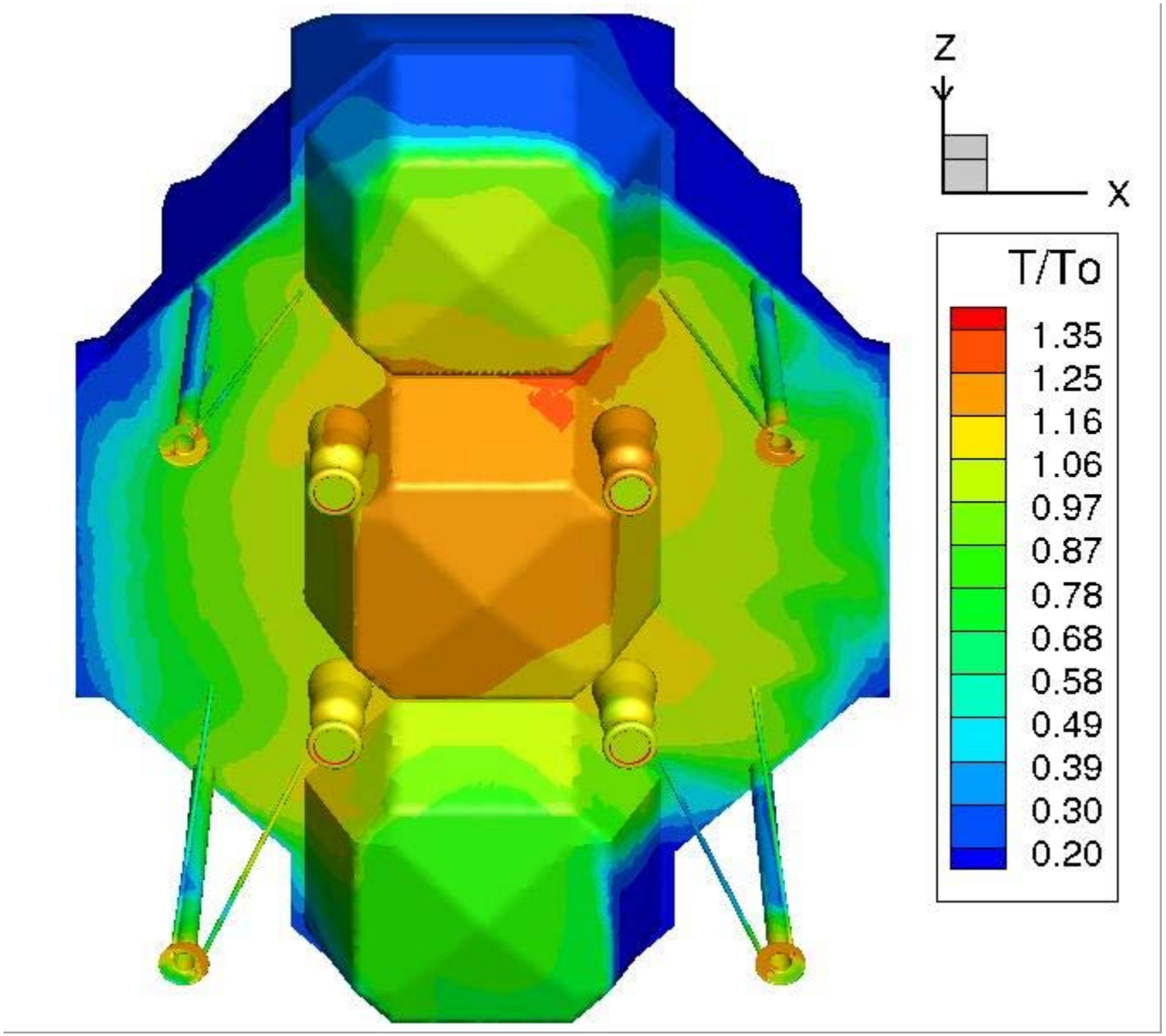

Base Radiative Heat Flux Contours

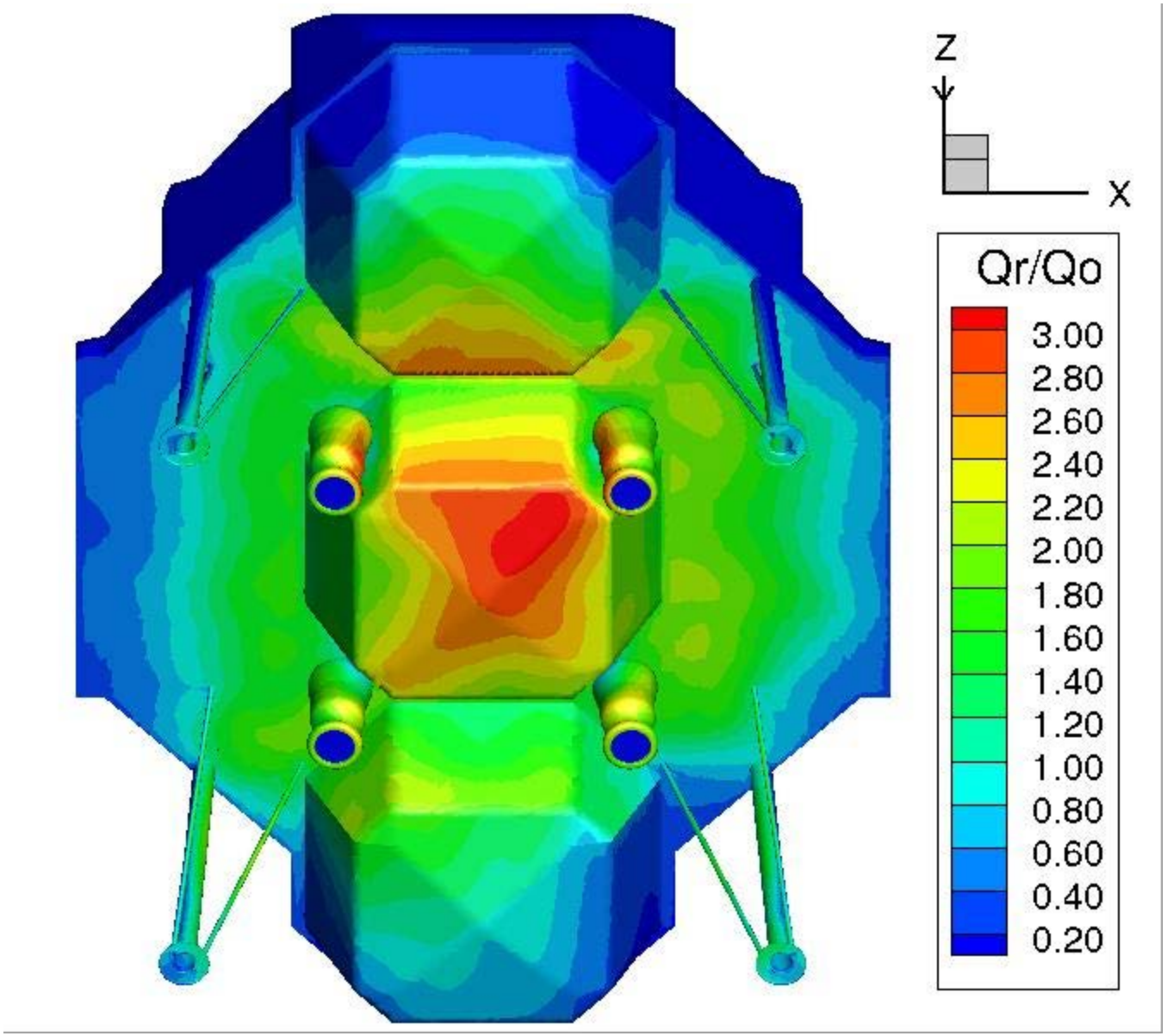

Factors for the asymmetric and unsteady flow

- Flow over uncovered components such as base domes, engines, and legs creates unsteady flows, which affects the fountain jet.
- Plume afterburning contributes to flow unsteadiness.
- The close proximity of the thruster plumes and pumping effect of the four nozzle jets can draw the weaker fountain jet off center and change the shape of the fountain jet (**Coanda effect**). The Coanda effect was not strong enough to cause the fountain jet to attach to the nozzle plumes.
- ANSA/AFLR generates predominately tetrahedral cells, resulting in asymmetry in the volume grid. Source cylinders helped center the fountain and nozzle jets, yet volume grid is still asymmetric.
- With an in-line 3 base-dome configuration and 2 pairs of engine each canted 3-deg outward in the +X and –X directions, lander geometry is symmetric about the Z-axis and X-axis, but not symmetric to the base center.
- CAD file was not perfectly symmetric

Example of the unsteady nature of the base flow

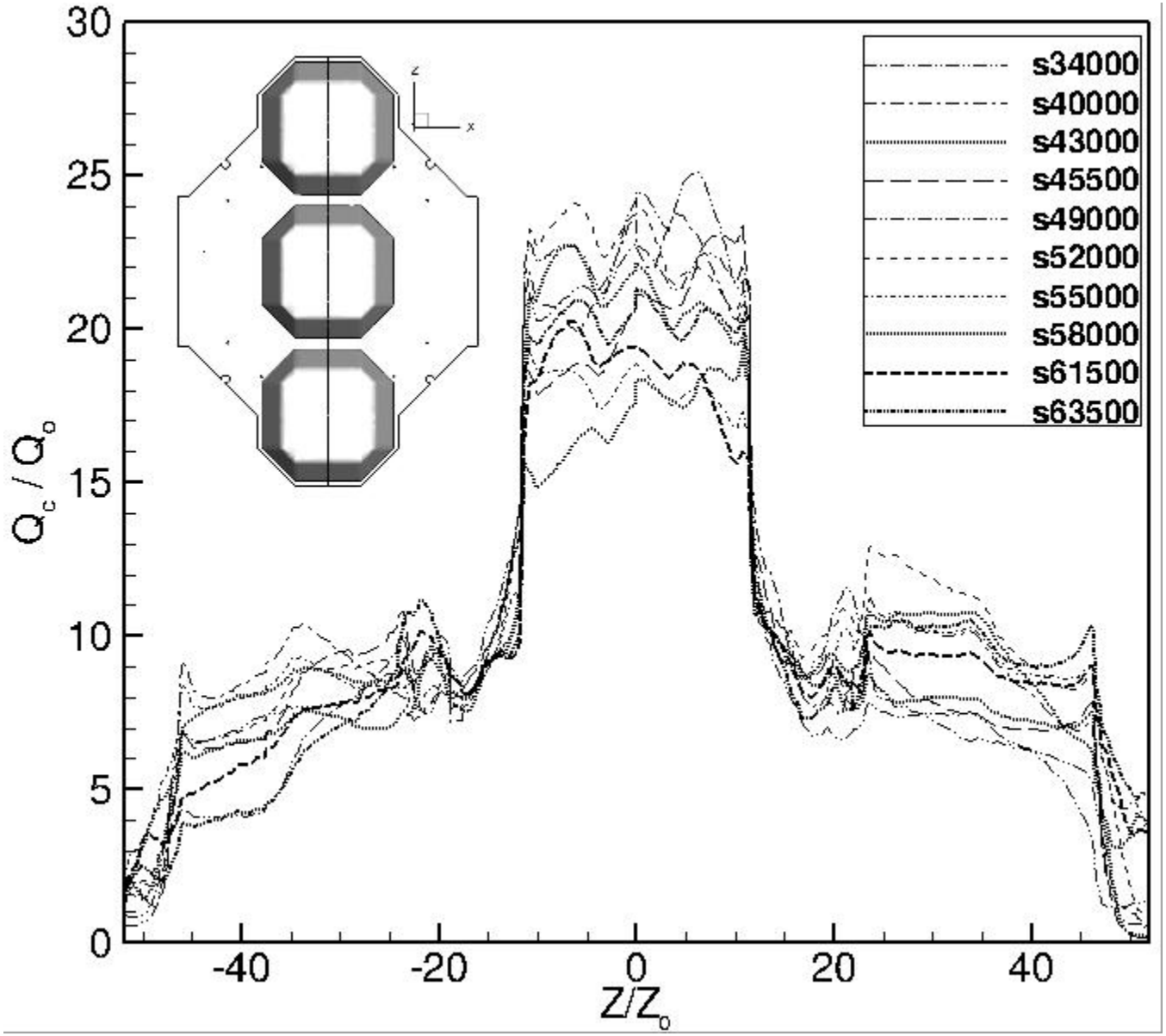

Example of the unsteady nature of the base flow

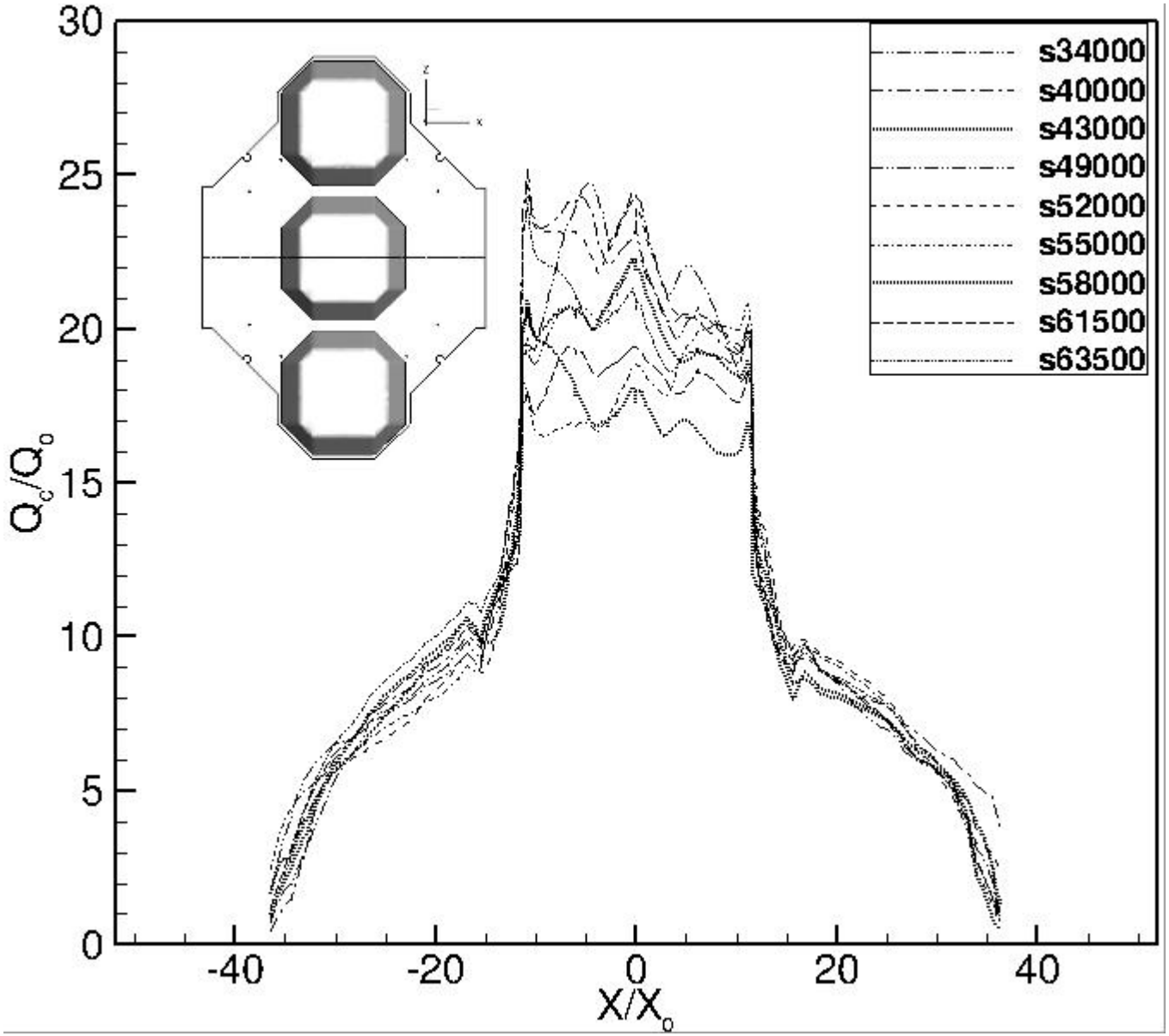

Comparison of computed radiative heat fluxes

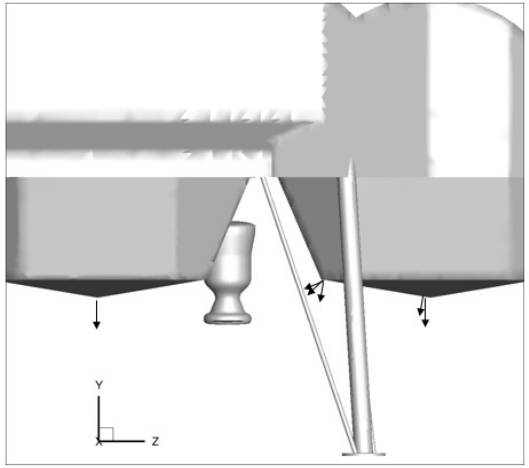

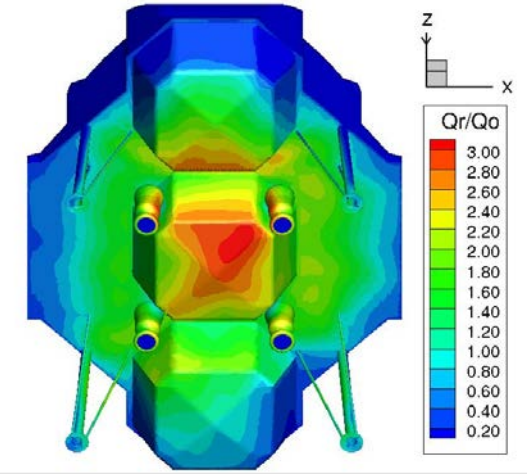

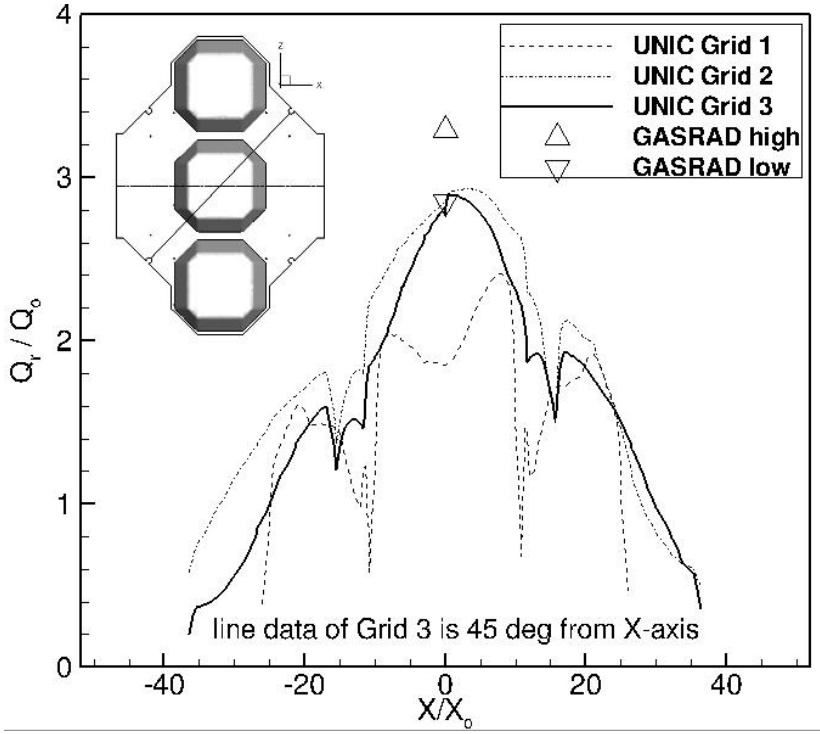

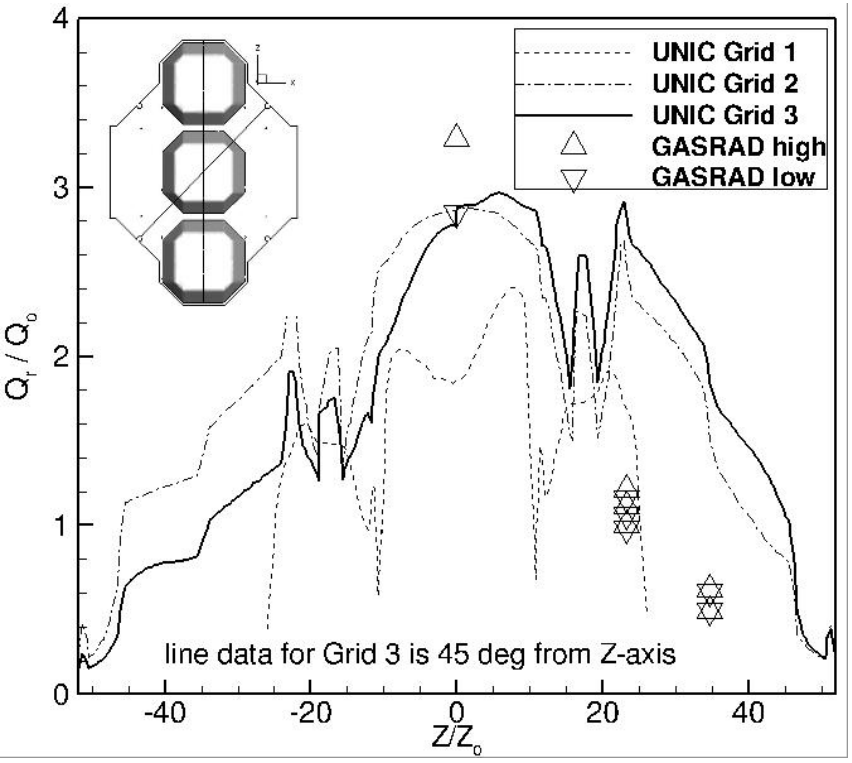

Comparison of peak base heat fluxes

	Grid	Qc/Qo	Qr/Qo
CFD non-reacting flow	1	16.5	-
	2	17.2	-
	3	16.7	-
CFD reacting flow	1	20.0	2.4
	2	22.6	2.9
	3	22.7	3.1
GASRAD	3	-	2.85~3.29

Results

Base heating environment for lunar lander hovering at a distance above the ground

Computational grid – Initial face meshes and source cylinders for Grid 4

- AFLR (Advancing Front Locally Reconnect) created volume cells that are inherently asymmetric. Source cylinder allows local cell refinement inside itself, providing better resolution for important flow regions such as fountain jet and nozzle jets.

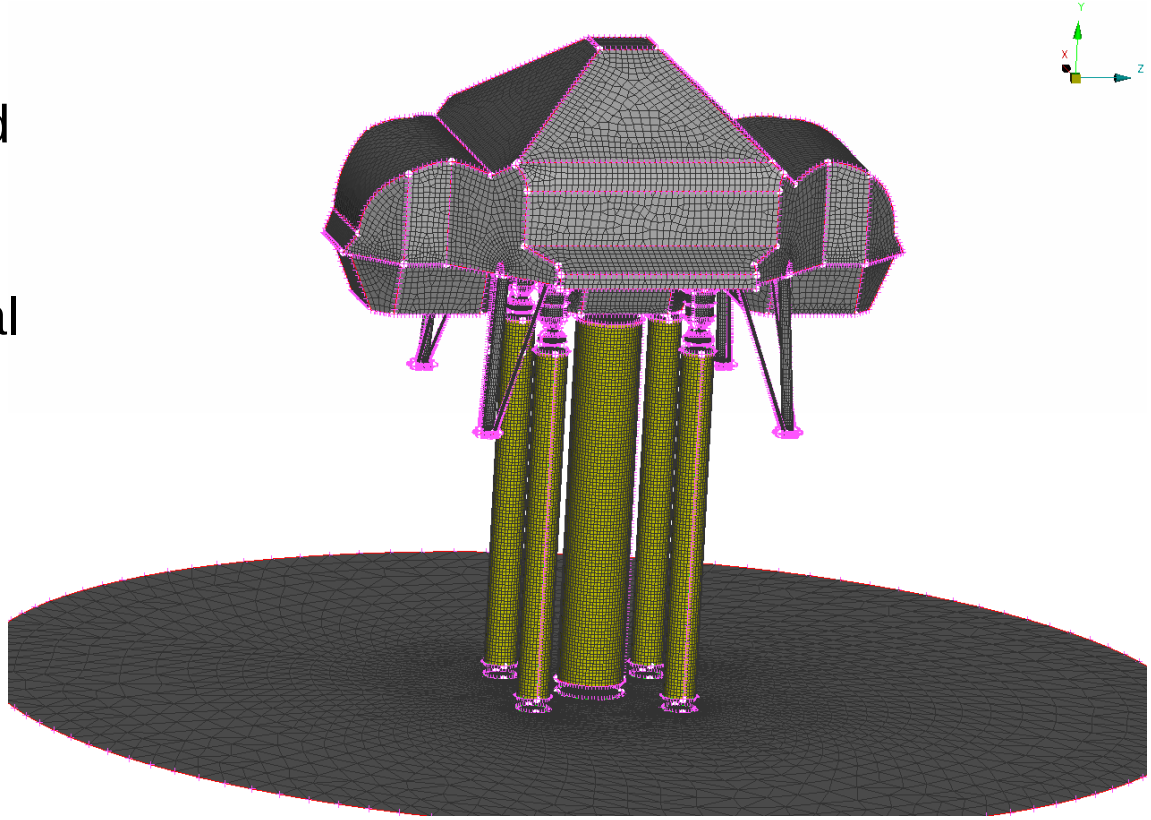

Grid 4: 16,983,366 cells

A Different Fountain Jet Physics For Hovering vs. On Pad

- At a distance above ground, the Coanda effect is prominent such that the fountain jet is attached to two of the four plumes and not impinging on base, resulting in a lower base heat flux. There are several factors that could lead to the strengthened Coanda effect:
  - The elongated plumes are less stable.
  - The plumes can expand more than those on pad, combining with the closeness of the nozzles, resulting in a more prominent Coanda effect.
  - The four nozzle are not symmetric to the center. Also the 3-degree canted nozzle outward in the +x and –x directions further weakens the strength of the plumes.

Plume and Fountain Jet Plot

- It can be seen that the weak fountain jet has attached to the two plumes at the +x direction.

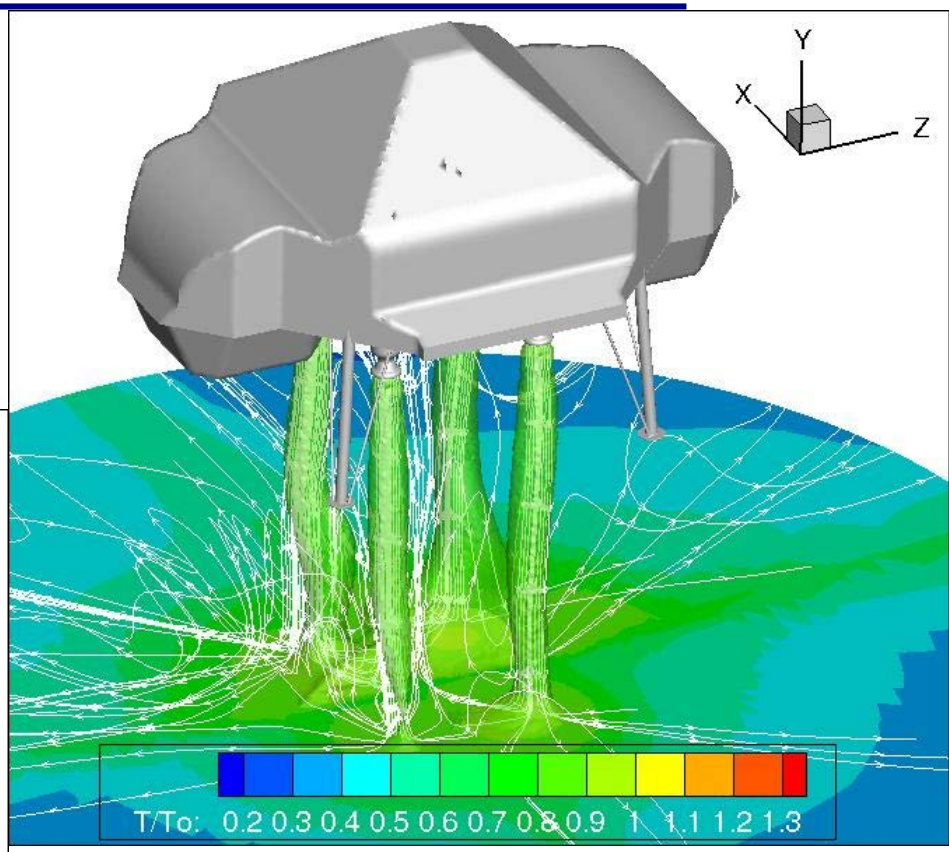

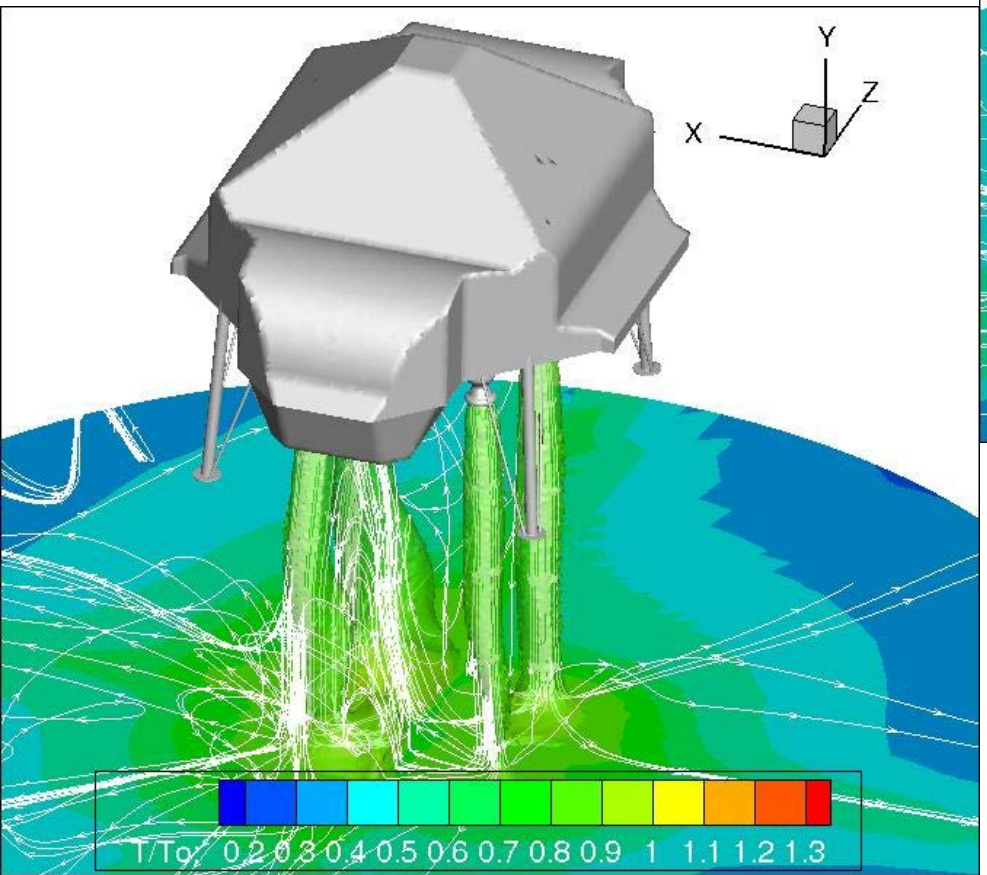

Q_c/Q_o Plot at Elapsed Times

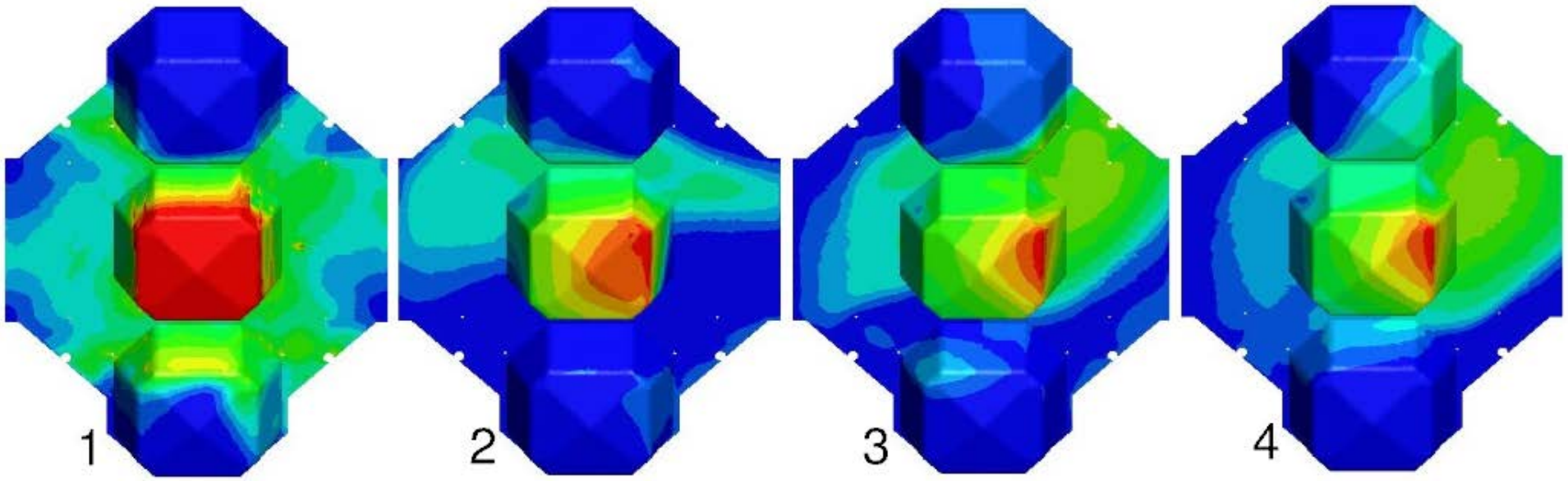

At frame 1, fountain jet was centered with a peak Qc/Qo~ 7.0. At frame 2, fountain jet was already attached to the two plumes in the +x-direction with a peak Qc/Qo ~ 5.3. **Once attached, the fountain jet never recovered back to base-center**. Peak Qc/Qo ~ 4.1 at frame 3 and ~ 5.3 at frame 4.

Comparison of Peak Base Heat Fluxes

	Base-to-ground Y/Yo	Grid	Qc/Qo	Qr/Qo
CFD non-reacting flow	1	1	16.5	-
	1	2	17.2	-
	1	3	16.7	-
CFD reacting flow	1	1	20.0	2.4
	1	2	22.6	2.9
	1	3	22.7	3.1
GASRAD	1	3	-	2.85~3.29
CFD reacting flow	4.3	4	5.3	0.9

Summary and Conclusions

- This study provided base heating environments for the testing of a four-engine lunar lander demonstrator on pad and hovering at a distance over ground, using an anchored computational methodology.
- Important near-ground base flow physics captured include the fountain jet, plume afterburning, nozzle plume-to-ground impingement, fountain jet-to-base impingement, base wall jet, and exhaust plume growth, due to differences in geometry and operating conditions.
- The Coanda effect prominently affected the fountain jet behaviors.
- When testing the lunar lander demonstrator on pad, the Coanda effect precursor makes the fountain jet oscillate about the central dome base, but the fountain jet itself never attached to any of the plumes. On the other hand, when the lunar lander demonstrator is hovering over ground, the Coanda effect forces the fountain jet to attach to two of the nozzle plumes, significantly reducing the base heat fluxes.

Summary and Conclusions - continued

- Convective heat fluxes are an order of magnitude greater than the radiative heat fluxes.
- Plume induced base heating environments for lunar lander demonstrator testing on pad indicate requirement of thermal protection system.
- Terrestrial lunar lander demonstrator plume induced environments are expected to be higher than those at vacuum.